Mechanistic and Kinetic Study of the Gas-Phase Reaction of Hydroxyl Radical with Dimethyl Sulfoxide

S. P. Urbanski,[†] R. E. Stickel,[‡] and P. H. Wine*[,†,‡,§]

School of Earth and Atmospheric Sciences, Georgia Tech Research Institute, School of Chemistry and Biochemistry, Georgia Institute of Technology, Atlanta, Georgia 30332

Received: August 18, 1998; In Final Form: October 19, 1998

Time-resolved tunable diode laser spectroscopic detection of CH_3, CH_4, and SO_2 has been coupled with 248 nm laser flash photolysis of H_2O_2 in the presence of $CH_3S(O)CH_3$ (DMSO) to study the mechanism and kinetics of the OH + DMSO reaction at 298 K. Production of CH_3 from the OH + DMSO reaction in the presence of N_2 buffer gas is observed. The rate-limiting step in CH_3 production is found to be the OH + DMSO reaction under all experimental conditions investigated (including first-order CH_3 production rates up to 10^5 s^{-1}), suggesting that a stabilized OH−DMSO adduct, if formed, has a lifetime of less than 10 μs toward methyl elimination at 298 K and 20 Torr total pressure. From measurements of the CH_3 appearance rate as a function of DMSO concentration, a rate coefficient of $k_1 = (8.7 \pm 1.6) \times 10^{-11}$ cm^3 $molecule^{-1}$ s^{-1} is obtained for the OH + DMSO reaction. Using the OH + CH_4 reaction as a "unit yield calibration", the CH_3 yield from OH + DMSO is found to be 0.98 ± 0.12. The uncertainties in k_1 and the CH_3 yield are 2σ and include estimates of systematic errors. Neither CH_4 nor SO_2 are observed as products of the OH + DMSO reaction. Upper limits (95% confidence limits) on the yields of CH_4 and SO_2 both in the presence and absence of O_2 are found to be 0.04 and 0.06, respectively. The atmospheric implications of our findings in the context of previous laboratory studies and atmospheric field measurements are discussed.

Introduction

Dimethyl sulfoxide ($CH_3S(O)CH_3$, DMSO) is an intermediate in the atmospheric oxidation of dimethyl sulfide (CH_3SCH_3, DMS). Dimethyl sulfide is produced via biological activity of phytoplankton in the ocean, and its release from the oceans is the largest natural source of atmospheric sulfur.[1−3] The gas-phase oxidation of DMS in the troposphere may play an important role in the global climate system because nonvolatile DMS oxidation products (the most important of which is H_2SO_4) have the ability to contribute to aerosol formation and growth in the remote marine environment.[4−6] By participating in the formation and growth of particles, DMS oxidation products may impact the earth−atmosphere radiation budget both directly, via aerosol extinction of solar radiation, and indirectly, by impacting cloud formation processes and thereby potentially influencing the distribution, lifetime, and optical properties of clouds. The current lack of knowledge regarding the DMS oxidation mechanism inhibits an accurate assessment of the importance of DMS as a source of various nonvolatile gases in the remote marine environment, a prerequisite to understanding the role of DMS in the global climate system.

In an attempt to better understand the DMS oxidation mechanism, we have examined a reaction involving the important intermediate dimethyl sulfoxide (DMSO). Dimethyl sulfoxide has been observed in the marine boundary layer[7−9] and has also been found to be a product of the OH-initiated oxidation of DMS in laboratory chamber studies.[10−12] The OH + DMS reaction proceeds via two separate channels, an O_2-independent channel and an O_2-dependent channel.[13−15] In 1 atm of air the channels have approximately equal rates at 285 K, with the O_2-dependent channel being favored at lower temperatures.[13] The O_2-dependent channel involves reversible addition of OH to DMS, forming the $CH_3S(OH)CH_3$ adduct. Reaction of $CH_3S(OH)CH_3$ with O_2 competes with adduct decomposition to reform OH and DMS.[13−15] The $CH_3S(OH)CH_3 + O_2$ reaction is presumed responsible for production of the DMSO observed in both the marine boundary layer[7−9] and in chamber studies[10−12] of the OH-initiated oxidation of DMS. The $CH_3S(OH)CH_3 + O_2$ reaction produces HO_2 with a yield of ca. 50%,[16,17] with the HO_2 being formed via abstraction of the hydroxyl H atom and DMSO presumably being formed as the HO_2 coproduct.[16,17]

In the atmosphere, the fate of DMSO is likely some combination of reaction with OH and physical removal (uptake by aerosol and cloud droplets in particular). The reaction of OH with DMSO has previously been the subject of three laboratory investigations. Barnes et al.[18] and Hynes and Wine[19] have both measured extremely fast rate coefficients for this reaction. The long-path FTIR study of Barnes et al.[18] observed the production of significant amounts of SO_2 as well as lesser amounts of dimethyl sulfone ($CH_3S(O)(O)CH_3$, $DMSO_2$), whereas another product study by Sorensen et al.[12] reported production of SO_2 and $DMSO_2$ in roughly equal amounts. The LFP−PLIF (laser flash photolysis−pulsed laser induced fluorescence) study of Hynes and Wine[19] also obtained some important mechanistic information; the rate coefficient was found to be independent of the pressure (25−700 Torr), isotopic identity of the hydrogen atoms in DMSO, i.e., H or D, and nature of the buffer gas (N_2 or O_2). Further, in contrast to the OH + DMS reaction, no evidence of reversible adduct formation was observed. The findings of Hynes and Wine[19] are consistent with OH addition to DMSO to form an adduct that does not

[†] School of Earth and Atmospheric Sciences.
[‡] Georgia Tech Research Institute.
[§] School of Chemistry and Biochemistry.

10.1021/jp9833911 CCC: $15.00
Published on Web 12/02/1998

TABLE 1. Elementary Reactions Which May Occur Following OH Attack on DMSO[a]

reaction		reaction no.
$OH + CH_3S(O)CH_3$	$\rightarrow CH_3S(O)CH_2 + H_2O$	1a
	$\rightarrow [CH_3S(O)(OH)CH_3]^* \rightarrow CH_3 + CH_3S(O)(OH)$	1b
(+ M)	$\rightarrow CH_3S(O)(OH)CH_3$	1c
$CH_3S(O)(OH)CH_3 + M$	$\rightarrow CH_3S(O)CH_2 + H_2O + M$	2a
	$CH_3 + CH_3S(O)(OH) + M$	2b
	$CH_4 + CH_3S(O)(O) + M$	2c
	$CH_4 + CH_3 + SO_2 + M$	2d
	$CH_3SO + CH_3OH + M$	2e
	other products	2f
$CH_3S(O)(OH)CH_3 + O_2$	$\rightarrow CH_3S(O)(O)CH_3 + HO_2$	3a
$CH_3S(O)(OH)CH_3 + O_2 + M$	$\rightarrow CH_3S(O_2)(O)(OH)CH_3 + M$	3b
$CH_3S(O_2)(O)(OH)CH_3 + M$	$\rightarrow CH_3S(O)(O)CH_3 + HO_2 + M$	4a
	$CH_3OO + CH_3S(O)(OH) + M$	4b
	$CH_3O + CH_3S(O)(O)(OH) + M$	4c
	$CH_4 + SO_2 + CH_3OO + M$	4d
	$CH_3O + CH_4 + SO_3 + M$	4e
	$CH_3 + CH_3OOH + SO_2 + M$	4f
	$CH_3S(O)(OH)CH_3 + O_2 + M$	4g
	other products	4h

[a] Oxygen-containing functional groups which appear in parentheses in reactions 1−4 (and elsewhere in the paper) are bound directly to sulfur.

decompose back to reactants on the time scale of their observations, i.e., 1−10000 μs. The lack of an observed isotope effect suggests that H-atom abstraction is only of minor importance in the OH + DMSO reaction.

The above-mentioned laboratory studies demonstrate that the OH-initiated oxidation of DMSO may contribute to SO_2 production in the marine layer boundary in addition to being the source of $DMSO_2$ that has been observed in atmospheric field measurements.[7−9] Elementary reactions which may occur following OH attack on DMSO are listed in Table 1. Oxygen-containing functional groups which appear in parentheses in reactions 1−4 (and elsewhere in the paper) are bound directly to sulfur.

The purpose of the current study is to clarify the mechanism of the OH + DMSO reaction by combining generation of OH radicals via laser flash photolysis with time-resolved detection of CH_3, CH_4, and SO_2 by tunable diode laser absorption spectroscopy (TDLAS). We have observed CH_3 production from the OH + DMSO reaction (in the absence of O_2), and using observed CH_3 infrared absorption temporal profiles, we have measured both the CH_3 yield and the OH + DMSO rate coefficient at 298 K. We have also placed upper limits on the yields of CH_4 and SO_2 from the OH + DMSO reaction both in the presence and absence of O_2. The atmospheric implications of our findings in the context of previous laboratory studies and atmospheric field measurements are discussed.

Experimental Section

The LFP-TDLAS technique used in this study was similar to that used in a number of previous studies of DMS oxidation carried out in our laboratory.[20−23] Excimer laser flash photolysis of H_2O_2 at 248 nm was employed to create OH radicals. In experiments where CH_3 production was monitored, H_2O_2/DMSO/N_2/CH_4 gas mixtures were used. Gas mixtures consisting of H_2O_2, DMSO, N_2, and in some cases O_2 were used in experiments designed to observe CH_4 and SO_2 production. A small amount (ca. 0.1 Torr) of C_2H_6 was included as a vibrational relaxer in the reaction mixtures when monitoring CH_4 production. Experimental conditions were such that the DMSO, CH_4, C_2H_6, and H_2O_2 were present in great excess over OH radicals, rendering the effects of radical−radical side reactions negligible.

The LFP−TDLAS apparatus has been described in detail elsewhere.[20−23] Only a brief description, including features unique to the present study, is included here. The infrared probe beam was generated by a lead-salt diode laser housed in a helium-cooled cryostat. Using a single-pass setup, the probe beam passed through the 1 m long reaction cell and entered a 0.5 m grating monochromator. Upon exiting the monochromator, the mode-selected infrared beam was detected using a HgCdTe infrared detector which was cooled to 77 K. A KrF excimer laser produced pulses of 248 nm photolysis radiation with an energy density in the reaction cell of ca. 5−30 mJ cm^{-2} and a duration of ca. 20 ns.

The H_2O_2 and DMSO were introduced into the gas mixture by bubbling a small flow of N_2 through the liquid and then mixing this flow into the carrier gas flow (N_2 or O_2 with CH_4 or C_2H_6 in some cases). The concentrations of both H_2O_2 and DMSO were measured in situ by UV photometry. The gas flow exiting the H_2O_2 bubbler was diluted with carrier gas prior to UV absorption monitoring at 253.7 nm using a Hg lamp and monochromator ($\sigma_{H_2O_2} = 7.0 \times 10^{-20}$ cm^2 $molecule^{-1}$).[24] After measurement of the [H_2O_2], this flow was added to the remainder of the gas flow (carrier gas and DMSO) and the entire reaction mixture was monitored by UV absorption at 213.9 nm (Zn lamp, 214 nm band-pass filters) upstream and downstream from the reaction cell. The absorption cross-sections used to convert 213.9 nm absorbances to concentrations were $\sigma_{DMSO} = 5.3 \times 10^{-18}$ cm^2 $molecule^{-1}$ [19] and $\sigma_{H_2O_2} = 3.2 \times 10^{-19}$ cm^2 $molecule^{-1}$.[24] Due to the low vapor pressure of DMSO (ca. 0.6 Torr at 298 K),[25] it was necessary to measure the [DMSO] both upstream and downstream from the reaction cell in order to quantify any loss of DMSO to the surfaces of the system. The [DMSO] measured exiting the reaction cell was typically 10−20% lower than the [DMSO] measured upstream from the reaction cell. The DMSO loss was greatest at the lowest linear flow rates. The impact of the uncertainties associated with the heterogeneous loss of DMSO to the walls of the reaction cell, the photometry cells, and the flow lines were minor and are discussed in the Results section of this paper. Downstream monitoring of the reaction mixture was conducted using a cross-shaped cell with long and short axes (long = 50.5 cm, short = 7.5 cm). This allowed for measurement of the [DMSO]

independent of any absorption caused by DMSO condensing on the photometry cell windows.

In experiments measuring the CH_3 appearance rate, the frequency of the diode laser (bandwidth $\approx 10^{-4}$ cm^{-1}) was tuned to the peak of the CH_3 absorption line at 606.12 cm^{-1}.[26] For experiments conducted to measure the CH_3 yield, the frequency of the probe beam was modulated by a 10 kHz sine-wave adjusted in amplitude for optimum second-harmonic detection of the absorption signal. In experiments designed to observe SO_2 (CH_4) production, the frequency of the probe beam was tuned over the SO_2 (CH_4) absorption line at 1347.00 cm^{-1} [27] (1303.71 cm^{-1})[27] by modulation (5−20 kHz) of the diode laser drive current. The absorption signal strength of the monitored species (CH_3, SO_2, or CH_4) was recovered from the digitized IR signal by subsequent computation of the second-harmonic Fourier amplitude in a few hundred intervals, each one a single modulation cycle in duration. The techniques used to calibrate the IR absorption signal for each species are described below in the pertinent sections.

One disadvantage of the of the TDLAS technique is the effect of pressure broadening of the absorption lines, which typically begins to degrade signal sensitivity around pressures of 25 Torr. Unfortunately, pressure broadening effects prevented us from conducting experiments at pressures above ca. 50 Torr. All of the experiments presented in this study were carried out at a 20−30 Torr total pressure.

The pure gases used in this study were obtained from Air Products Specialty Gases (N_2, O_2), Matheson Gas Products (OCS, NO_2, SO_2, HBr), and Spectra Gases (C_2H_6, CH_4) and had the following stated minimum purities: N_2, 99.999%; O_2, 99.99%; OCS, 97.5%; NO_2, 99.5%; SO_2, 99.98%; C_2H_6, 99.97%; CH_4, 99.995%. The N_2, O_2, CH_4, SO_2, and C_2H_6 were used as supplied. The OCS was filtered through ascarite and degassed at 77 K. The NO_2 was transferred to a Pyrex bulb and diluted with O_2. The HBr was repeatedly degassed at 77 K prior to use. Dimethyl sulfoxide (Sigma Aldrich HPLC) and methyl iodide were acquired from Aldrich Chemical Corp. and had stated minimum purities of 99.9% and 99.5%, respectively. Hydrogen peroxide (50% H_2O_2 in H_2O) was acquired from Fisher Scientific. The dimethyl sulfoxide was transferred under nitrogen into a Pyrex bubbler fitted with high-vacuum stopcocks. The methyl iodide was transferred to a dark vial fitted with a high-vacuum stopcock and was degassed at 77 K repeatedly before use.

Results

Methyl Production Rate. When H_2O_2 was photolyzed in the presence of DMSO, methyl radical formation was observed. Methyl was not observed in the absence of H_2O_2. The rate of methyl formation was found to be dependent on the [DMSO], and the magnitude of the peak CH_3 IR absorbance varied linearly with the [H_2O_2] and UV fluence. These observations indicate that the observed CH_3 production resulted from the reaction of OH radicals with DMSO and that CH_3 generation from DMSO photolysis was not significant. The CH_3 temporal profiles were analyzed using a nonlinear least-squares fit to the sum of an exponential rise and an exponential decay (see Figure 1). The double-exponential functional form included four variable parameters: a first-order CH_3 appearance rate (k_a), a first-order CH_3 disappearance rate (k_d), the CH_3 signal at infinite time in the absence of any CH_3 loss (S_0), and the time of OH generation (t_0). In our experiments, CH_3 disappearance results primarily from CH_3 self-reaction and is not strictly a first-order loss process. The variable for first-order CH_3 disappearance, k_d, is

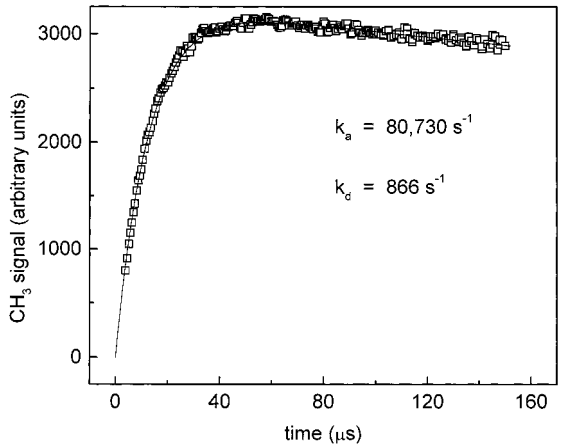

Figure 1. Typical CH_3 IR absorption temporal profile observed following 248 nm laser flash photolysis of a H_2O_2/DMSO/CH_4/N_2 mixture and the double-exponential fit to the data. Data acquired at 20 Torr total pressure and 298 K. Laser fluence of ca. 32 mJ cm^{-2} pulse^{-1}, 320 laser shots averaged. Concentrations in units of molecule cm^{-3} are [H_2O_2] = 1.6×10^{15}, [DMSO] = 8.4×10^{14}, [CH_4] = 2.0×10^{17}, [OH]$_0$ = 1.2×10^{13}.

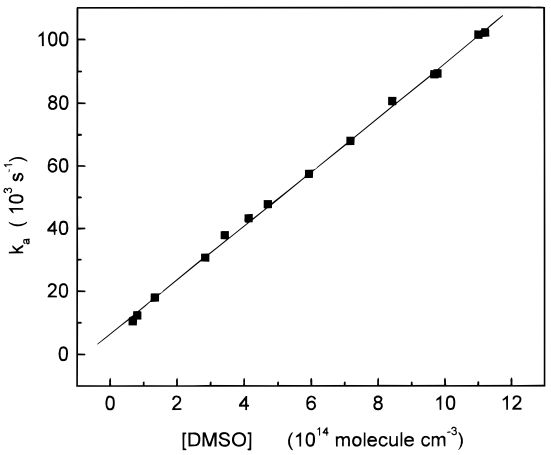

Figure 2. Pseudo-first-order rate coefficient (k_a) versus [DMSO] for the OH + DMSO reaction at 298 K and 20 Torr total pressure (including ca. 6 Torr of CH_4). The solid line is a linear least-squares fit. The best-fit slope is $(8.6 \pm 0.2) \times 10^{-11}$ cm^3 molecule^{-1} s^{-1}, where the uncertainty is 2σ and represents precision only.

thus a parametrized CH_3 disappearance rate coefficient rather than the sum of actual loss processes which are quantitatively attributable to specific first-order reactions. Because the CH_3 loss rates are very slow compared to the rapid rate of CH_3 appearance, the parametrization of the CH_3 disappearance as a first-order process does not impact the integrity or reliability of the analysis. As may be seen in Figure 1, the quality of the fits is excellent.

$$S(t) = S_0[\exp^{-k_d(t-t_0)} - \exp^{-k_a(t-t_0)}] \qquad \text{(I)}$$

Plots of k_a vs [DMSO] are linear over the range of [DMSO] employed (see Figure 2). The linearity of the k_a vs [DMSO] plot up to the fastest appearance rate measured (ca. 100 000 s^{-1}) demonstrates that the rate-limiting step in methyl production is the OH + DMSO reaction under all experimental conditions investigated; hence, the lifetime of a $CH_3S(O)(OH)CH_3$ adduct is less than 10 μs at room temperature and 20 Torr total pressure. The CH_3 appearance rate was independent of [H_2O_2], [OH]$_0$, and UV fluence, showing that CH_3 formation via DMSO-independent channels was not significant in these experiments.

The slope of the k_a vs [DMSO] plot (see Figure 2) yields the second-order rate coefficient $k_1 = (8.6 \pm 0.2) \times 10^{-11}$ cm^3 molecule^{-1} s^{-1} at 298 K and 20 Torr total pressure, where the uncertainty is 2σ and represents precision only.

Experiments were conducted in both the absence and presence of methane in order to discern any impact that relaxation of vibrationally excited CH_3 radicals may have had on the observed CH_3 temporal profiles. In the current study, photolysis of CH_3I at 248 nm in the presence of varying amounts of CH_4 demonstrated that CH_4 is an effective relaxer of vibrationally excited CH_3 radicals. The rate coefficient measured in the presence of 6 Torr of CH_4 (Figure 2) is equal, within experimental error, to that measured in the absence of CH_4 ($k_1 = (8.9 \pm 0.2) \times 10^{-11}$ cm^3 molecule^{-1} s^{-1}), demonstrating that relaxation of excited CH_3 radicals is unimportant in our measurement of the OH + DMSO rate coefficient. The values of k_1 were determined using the average of the [DMSO] measured upstream and downstream from the reaction cell. The values of k_1 determined in this manner differed by only ±5% from the values of k_1 determined using only the upstream or downstream measurement of the [DMSO]. The greatest uncertainty in our measurement of the OH + DMSO rate coefficient is the DMSO absorption cross section used for the in situ measurement of [DMSO] ($\sigma_{DMSO} = (5.3 \pm 1.0) \times 10^{-18}$ cm^2 molecule^{-1} at 213.9 nm).[19] Consideration of this uncertainty leads us to report an OH + DMSO rate coefficient of $k_1 = (8.7 \pm 1.6) \times 10^{-11}$ cm^3 molecule^{-1} s^{-1} at 298 K and 20 Torr total pressure; this value is a weighted average of the experiments conducted in both the presence and absence of CH_4.

Methyl Yield. The CH_3 yield from the OH + DMSO reaction was determined by comparison of CH_3 levels observed from the OH + DMSO reaction with levels observed from the OH + CH_4 reaction:

$$OH + CH_4 \rightarrow CH_3 + H_2O \qquad (5)$$

The OH + CH_4 reference reaction was chosen because it is the only thoroughly studied reaction of OH known to produce CH_3 with unit yield.[24] Hydrogen peroxide was photolyzed in ca. 30 Torr of CH_4, both in the absence and presence of DMSO. Because the OH + H_2O_2 reaction (reaction 6) is 200 times faster than the OH + CH_4 reaction, 30 Torr of CH_4 was necessary to adequately minimize OH loss via reaction with H_2O_2.

$$OH + H_2O_2 \rightarrow HO_2 + H_2O \qquad (6)$$

The OH + DMSO reaction was also studied in 30 Torr of CH_4 in order to maintain the same line-broadening environment for CH_3 observation. Without DMSO present, the removal of OH by CH_4 is complete in ca. 400 μs (see Figure 3). With DMSO present, the OH is removed by reactions with DMSO and CH_4 within 10−200 μs, depending on the DMSO concentration. In both the absence and presence of DMSO, the loss of CH_3 radicals is primarily due to the CH_3 self-reaction:

$$CH_3 + CH_3 + M \rightarrow C_2H_6 + M \qquad (7)$$

Hence, the time dependence of the CH_3 decay is described by the following equation

$$\frac{1}{S_t} = \frac{1}{S_0} + 2k_7 t \qquad (II)$$

where S_0 is the CH_3 signal which would be observed at infinite time if there were no CH_3 loss processes.

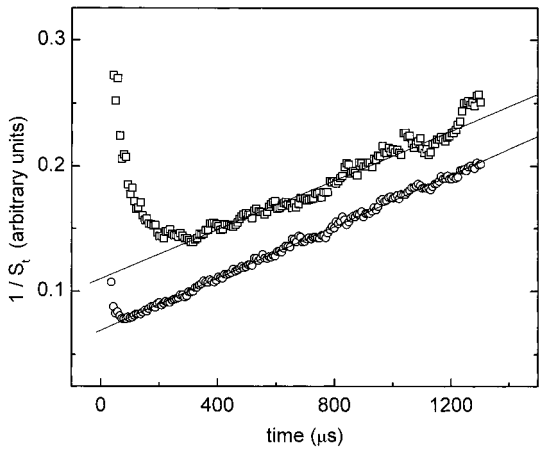

Figure 3. Typical CH_3 infrared absorption profiles plotted as 1/signal (1/S) versus time. Data acquired via 248 nm laser flash photolysis of $H_2O_2/CH_4/N_2$ gas mixtures in the presence (○) and absence (□) of DMSO. Total pressure = 30 Torr, and T = 298 K. Symbols are experimental data. Lines are linear least-squares fits. Concentrations in units of molecule cm^{-3} are (□) $[H_2O_2] = 2.0 \times 10^{15}$, $[CH_4] = 9.4 \times 10^{17}$, $[OH]_0 = 1.6 \times 10^{13}$, (○) $[DMSO] = 4.3 \times 10^{14}$, $[H_2O_2] = 2.2 \times 10^{15}$, $[CH_4] = 9.3 \times 10^{17}$, $[OH]_0 = 1.8 \times 10^{13}$. Best-fit intercepts ($1/S_0$) are, in arbitrary units, (□) 0.103 and (○) 0.068. See text and eqs II and III for methyl yield determination from the data.

The value of S_0 for each individual experiment was determined by a linear least-squares analysis of the $1/S_t$ vs time plot, disregarding the portion of the plot when CH_3 production was still occurring (see Figure 3). The S_0 from the reference experiments, S_0', and from experiments with DMSO, S_0'', were used in the following equation to determine the CH_3 yield from the OH + DMSO reaction:

$$\Phi = \frac{\left(\frac{S_0'' k'' U' [H_2O_2]'}{S_0' k' U'' [H_2O_2]''} k_5 [CH_4]'\right) - k_5 [CH_4]''}{k_1 [DMSO]''} \qquad (III)$$

In the above equation, k'' and k' represent the first-order loss rates for OH radicals, i.e.:

$$k'' = k_1[DMSO]'' + k_5[CH_4]'' + k_6[H_2O_2]''$$

$$k' = k_5[CH_4]' + k_6[H_2O_2]'$$

Variation in the UV fluence is accounted for by the U' and U'' terms. Second-order rate coefficients are, in units of cm^3 molecule^{-1} s^{-1}, $k_5 = 6.3 \times 10^{-15}$;[24] $k_6 = 1.7 \times 10^{-12}$;[24] $k_1 = 8.4 \times 10^{-11}$. The value used for k_1 is an average of the rate coefficients reported in refs 18 and 19 and in the current study.

The results of our methyl yield measurements are summarized in Figure 4. The data render a CH_3 yield of approximately unity ($\Phi(CH_3) = 0.98 \pm 0.08$, where the uncertainty represents 2σ, precision only). As may be seen in Figure 4, the measured CH_3 yields were independent of the DMSO concentration, confirming that DMSO photolysis was unimportant in producing CH_3 under the conditions of our experiments. The CH_3 yields determined from our data were virtually insensitive to uncertainties in both the OH + DMSO rate coefficient and the DMSO UV absorption cross section used for in situ determination of [DMSO] ($\sigma_{DMSO} = (5.3 \pm 1.0) \times 10^{-18}$ cm^2 molecule^{-1} at 213.9 nm).[19] Uncertainties associated with the loss of DMSO to the walls of the reaction cell, photometry cells, and flow lines had no effect on the CH_3 yields. We believe the systematic errors associated with our measurement of the CH_3 yield are small. However, we allow for the possibility of unknown systematic errors by

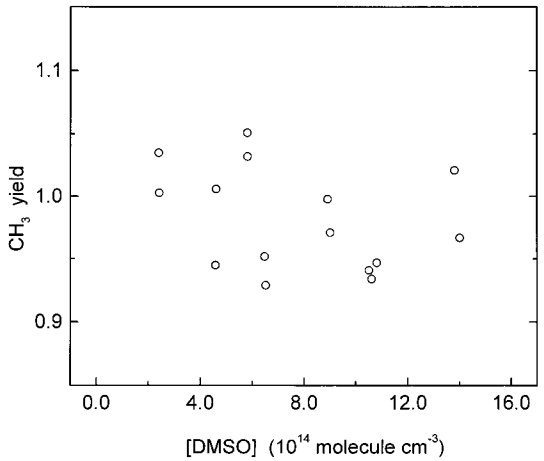

Figure 4. Observed CH_3 yield from OH + DMSO at $T = 298$ K and $P = 30$ Torr CH_4. Methyl yield plotted versus [DMSO]. Average of data gives a CH_3 yield of 0.98 ± 0.08, where the uncertainty is 2σ and represents precision only.

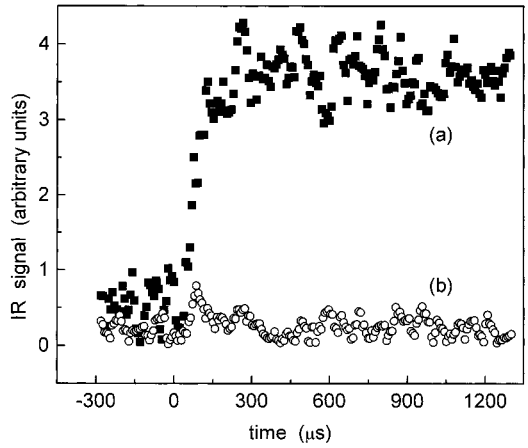

Figure 5. Typical second-harmonic infrared signal profiles obtained by tuning the frequency of the probe beam over the CH_4 absorption line at 1303.71 cm^{-1}. (a) Photolysis of $CH_3I/HBr/H_2O_2/C_2H_6/N_2$ mixture at $T = 297$ K and $P = 20$ Torr; laser fluence of 4.8 mJ cm^{-2} $pulse^{-1}$, 32 laser shots averaged. (b) Photolysis of $DMSO/H_2O_2/C_2H_6/N_2$ mixture at $T = 297$ K and $P = 20$ Torr; laser fluence of 24.4 mJ cm^{-2} $pulse^{-1}$, 32 laser shots averaged. Concentrations in units of molecule cm^{-3} are (a) $[CH_3I] = 2.4 \times 10^{14}$, $[HBr] = 3.6 \times 10^{15}$, $[H_2O_2] = 1.2 \times 10^{15}$, $[C_2H_6] = 3.2 \times 10^{15}$, $[CH_3]_0 = 1.2 \times 10^{12}$, $[OH]_0 = 1.3 \times 10^{12}$; (b) $[H_2O_2] = 1.5 \times 10^{15}$, [DMSO] $=1.3 \times 10^{15}$, $[C_2H_6] = 4.0 \times 10^{16}$, $[OH]_0 = 8.3 \times 10^{12}$. The CH_4 IR signal depicted in (a) corresponds to a CH_4 yield of ca. 15% from OH + DMSO under the conditions employed to obtain data in b.

increasing the uncertainty of our yield measurement, leading us to report $\Phi(CH_3) = 0.98 \pm 0.12$. Room-temperature yield measurements were also conducted at 10 Torr total pressure (including ca. 8 Torr of CH_4) using CH_3I photolysis to calibrate the CH_3 IR absorption signal. The 10 Torr results are consistent with (though less precise than) the higher pressure CH_3 yield measurements, with $\Phi(CH_3) = 1.02 \pm 0.16$ (error represents 2σ, precision only).

Methane Production. Methane was not observed as a product of the OH + DMSO reaction in either N_2 or O_2 buffer gas. The CH_3 + HBr reaction produces CH_4 in unit yield[28] and was used to confirm our ability to readily detect CH_4 production and to calibrate the CH_4 IR absorption signal at 1303.71 cm^{-1}. The CH_4 IR absorption signal calibration was carried out by photolyzing ($\lambda = 248$ nm) gas mixtures containing HBr, CH_3I, H_2O_2, C_2H_6, and N_2. Because H_2O_2 possesses strong infrared absorption features in the 1300 cm^{-1} spectral region,[27] it was included in the calibration gas mixtures to demonstrate that its presence did not interfere with CH_4 detection. The concentrations of HBr, CH_3I, H_2O_2, and C_2H_6 and the excimer laser fluence were adjusted to ensure that the following conditions were satisfied: (1) CH_3 radicals reacted almost exclusively with HBr; (2) the fate of the OH radicals was reaction with HBr, H_2O_2, and C_2H_6; (3) the $[C_2H_6]$ was sufficient to ensure rapid relaxation of vibrationally excited CH_4. The $[CH_3]_0$ and hence peak $[CH_4]$ was calculated from the $[CH_3I]$ (measured in situ by UV photometry at 253.7 nm), the CH_3I absorption cross section at 248 nm ($\sigma_{248} = 81.5 \times 10^{-20}$ cm^2 $molecule^{-1}$, $\sigma_{254} = 110 \times 10^{-20}$ cm^2 $molecule^{-1}$, both measured as part of the current study and in excellent agreement with recently published measurements),[29] and the UV fluence. The accuracy of this calibration was verified by CH_4 standard addition, achieved using a certified custom gas blend obtained from Scott Specialty Gases (150.9 ppm CH_4 in N_2; grade Acublend Master Gas, analytical accuracy = ±1%). Plots of $[CH_3]_0$ vs peak CH_4 IR signal were linear and a linear least-squares fit to the data yielded the CH_4 IR absorption signal calibration.

No evidence of CH_4 production was observed when examining the OH + DMSO reaction. Figure 5 shows typical data from CH_3 + HBr and OH + DMSO experiments. Using the CH_4 IR absorption signal calibrations, upper limits on CH_4 yields were obtained for the data acquired from the OH + DMSO experiments in both N_2 and O_2 buffer gases. The upper limits for the CH_4 yields derived from the data are (95% confidence limits) 0.039 in N_2 buffer gas and 0.038 in O_2 buffer gas. Both upper limits were obtained at 20 Torr total pressure and room temperature. Uncertainties associated with the loss of DMSO to the walls of the reaction cell, photometry cells, and flow lines had no effect on the upper-limit CH_4 yields.

Sulfur Dioxide Production. Sulfur dioxide was not observed as a product of the OH + DMSO reaction in either N_2 or O_2 buffer gas. The ability of our system to detect small concentrations of SO_2 in time-resolved experiments was verified by photolyzing OCS in the presence of O_2 and NO_2, which generates SO_2 via to the following set of reactions:

$$OCS + h\nu \rightarrow S + CO \qquad \Phi(CO) \approx 1^{30} \tag{8}$$

$$S + O_2 \rightarrow SO + O \qquad k = 2.8 \times 10^{-12}\ cm^3\ molecule^{-1}\ s^{-1}\ ^{31} \tag{9}$$

$$S + NO_2 \rightarrow SO + NO \qquad k = 6.5 \times 10^{-11}\ cm^3\ molecule^{-1}\ s^{-1}\ ^{31} \tag{10}$$

$$SO + NO_2 \rightarrow SO_2 + NO \qquad k = 1.4 \times 10^{-11}\ cm^3\ molecule^{-1}\ s^{-1}\ ^{32} \tag{11}$$

The SO + O_2 reaction is too slow to be important for the $[O_2]$ employed in our experiments.[24] The study of Zhao et al.[30] has established that OCS photolysis at 248 nm produces CO and S atoms in approximately unit yield, and Sivakumar et al.[33] have shown that $S(^1D_2)$ is the only sulfur fragment generated by OCS photolysis at this wavelength. For the conditions employed in our study, ≳99% of $S(^1D_2)$ atoms are quenched to $S(^3P_J)$,[34] with the remainder reacting with OCS to form S_2 + CO.[35] By using sufficient NO_2 and O_2 ($[NO_2] \approx 1.5 \times 10^{15}$ molecule cm^{-3}; $[O_2] \approx 2.6 \times 10^{16}$ molecule cm^{-3}) and low excimer laser fluence (typically ≲ 8 mJ cm^{-2} in the reaction cell), we were able to ensure that the following conditions were satisfied: (1) the S atoms generated by OCS photolysis reacted predominantly with

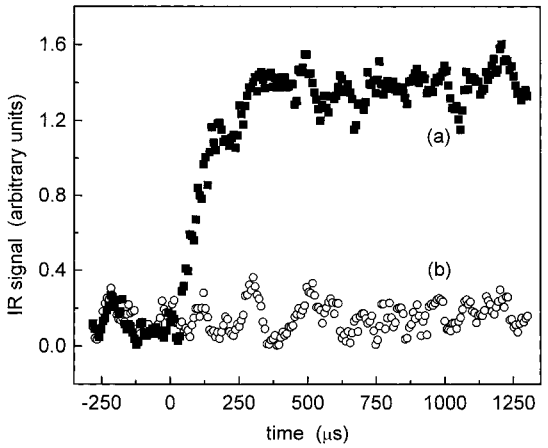

Figure 6. Typical second-harmonic infrared signal profiles obtained by tuning the frequency of the probe beam over the SO_2 absorption line at 1347.000 cm^{-1}. (a) Photolysis of $OCS/NO_2/O_2/N_2$ mixture at $T = 295$ K and $P = 32$ Torr; laser fluence of 13.4 mJ cm^{-2} $pulse^{-1}$, 32 laser shots averaged. (b) Photolysis of $DMSO/H_2O_2/O_2/N_2$ mixture at 295 K and 31 Torr; laser fluence of 22 mJ cm^{-2} $pulse^{-1}$, 32 laser shots averaged. Concentrations in units of molecule cm^{-3} are (a) $[OCS] = 6.4 \times 10^{15}$, $[NO_2] = 1.5 \times 10^{15}$, $[O_2] = 2.2 \times 10^{16}$, $[S]_0 = 2.3 \times 10^{12}$; (b) $[DMSO] = 5.4 \times 10^{14}$, $[H_2O_2] = 2.4 \times 10^{15}$, $[O_2] = 9.1 \times 10^{17}$, $[OH]_0 = 1.2 \times 10^{13}$. The SO_2 IR signal depicted in (a) corresponds to an SO_2 yield of ca. 19% from OH + DMSO under the conditions employed to obtain data in b.

O_2 or NO_2, producing SO (and O or NO); (2) the fate of O atoms produced by reaction 9 was scavenging by NO_2; (3) SO produced in reactions 9 and 10 reacted almost exclusively with NO_2 (reaction 11); (4) generation of SO_2 was rapid compared to SO_2 diffusional losses. When these conditions are satisfied, the $[S]_0$ is equal to the peak SO_2 concentration. Under typical conditions in our study, ca. 95% of the S atoms are converted into SO_2 via reactions 9−11, with the balance being converted to S_2 by reaction with OCS. By varying the OCS concentration and the excimer laser fluence, we were able to calibrate the SO_2 IR absorption signal at 1347.00 cm^{-1}. Plots of $[S]_0$ vs peak SO_2 IR absorption signal were linear, and a linear least-squares fit to the data yielded the SO_2 IR absorption signal calibration. The $[S]_0$ was calculated using the measured UV fluence, the OCS absorption cross section at 248 nm, and the OCS concentration measured in situ at 213.9 nm ($\sigma_{248} = 2.11 \times 10^{-20}$ cm^2 $molecule^{-1}$, $\sigma_{213.9} = 21.8 \times 10^{-20}$ cm^2 $molecule^{-1}$).[24] No evidence for SO_2 production was observed when examining OH + DMSO. Figure 6 presents typical data from $OCS + O_2 + NO_2 + h\nu$ and $H_2O_2 + DMSO + O_2 + h\nu$ experiments. Utilizing the SO_2 IR absorption signal calibrations, upper limits on SO_2 yields were determined for the data acquired from the OH + DMSO experiments in both N_2 and O_2 buffer gases. The upper-limit SO_2 yields defined by the data are (95% confidence limits) 0.055 in N_2 buffer gas and 0.062 in O_2 buffer gas. Both upper limits were obtained at 30 Torr total pressure and room temperature. The upper limit SO_2 yields were determined using the [DMSO] measured downstream from the reaction cell and are ca. 5% higher than the upper limits defined by the upstream [DMSO] measurement (0.053 in N_2 buffer and 0.060 in O_2 buffer).

Discussion

The data presented in this paper demonstrate that, in the absence of O_2, the OH + DMSO reaction produces CH_3 in unit yield. In addition, we find that if a stabilized $CH_3S(O)(OH)CH_3$ adduct is formed, its lifetime toward decomposition to CH_3 is less than 10 μs at 20 Torr and 298 K. The room-temperature rate coefficient for the OH + DMSO reaction, as derived from CH_3 appearance data, is $k_1 \pm 2\sigma = (8.7 \pm 1.6) \times 10^{-11}$ cm^3 $molecule^{-1}$ s^{-1}. The relatively large error bar results from uncertainties in the DMSO UV absorption cross section used for the in situ photometric measurements of the DMSO concentration. Methane and SO_2 were not observed as products of the OH + DMSO reaction in either N_2 or O_2 buffer gas.

In the absence of O_2, the observed unit yield of CH_3 and the near-zero yields of CH_4 and SO_2 lead us to conclude that the dominant OH + DMSO reaction channel is characterized by OH addition to DMSO, followed by rapid $CH_3S(O)(OH)CH_3$ adduct decomposition to CH_3 and $CH_3S(O)(OH)$ (methane sulfinic acid, MSIA), i.e., reaction 1b *or* reaction 1c followed by reaction 2b. We have not directly observed MSIA but have arrived at the conclusion that MSIA is the CH_3 coproduct by the process of elimination. Our observations demonstrate that other prospective reaction mechanisms, e.g. 1a, 2a, 2c−f, are not significant for the conditions of our experiments. Our results verify the proposal of Yin et al.,[36] who suggested based on smog chamber studies, bond dissociation energy (BDE) calculations, and analogy with liquid-phase chemistry that the OH + DMSO reaction occurs via OH addition, followed by C−S bond cleavage, in contrast to the OH + DMS reaction which is characterized by H-atom abstraction and reversible adduct formation. The source of the difference in OH reaction mechanisms between DMS and DMSO lies in the C−S BDEs. Because the C−S BDE in DMS (308.4 ± 5.0 kJ mol^{-1})[24,37] is significantly larger than the C−S BDE in DMSO (236.0 ± 16.7 kJ mol^{-1}),[24,37] CH_3 elimination from OH + DMSO is exothermic by 101 ± 28 kJ mol^{-1},[24,37] whereas CH_3 elimination from OH + DMS is endothermic by 55 ± 26 kJ mol^{-1}.[24,37]

The observed unit yield of methyl in the current study is consistent with the findings of Hynes and Wine[19] in which the OH + DMSO reaction was studied using PLIF to monitor the disappearance of OH radicals. Hynes and Wine did not observe a kinetic isotope effect when using deuterated DMSO, indicating that reaction 1 does not proceed by H-atom abstraction to any significant extent. Additionally, Hynes and Wine saw no evidence that the adduct decomposed back to reactants. The room-temperature rate coefficient measured here falls between the only two published measurements: $k_1 = (1.0 \pm 0.3) \times 10^{-10}$ cm^3 $molecule^{-1}$ s^{-1} [19] and $k_1 = (6.5 \pm 2.5) \times 10^{-11}$ cm^3 $molecule^{-1}$ s^{-1}.[18]

While we have high confidence in the results presented here, direct application of our results to the atmosphere is somewhat tenuous. Due to reaction between CH_3 and O_2, we were unable to employ CH_3 observations to assess the ability of the $CH_3S(O)(OH)CH_3 + O_2$ reaction to compete with adduct decomposition to CH_3 and $CH_3S(O)(OH)$. Smog chamber studies examining the OH + DMSO reaction in an 1 atm of air indicate that under such conditions 20−30% of the oxidized DMSO is converted to dimethyl sulfone ($CH_3S(O)(O)CH_3$, $DMSO_2$);[12,18] these studies provide evidence for the occurrence of a $CH_3S(O)(OH)CH_3 + O_2$ reaction that produces $CH_3S(O)(O)CH_3 + HO_2$, i.e., a reaction analogous to that responsible for DMSO production from the OH + DMS + O_2 system.[10−12,16,17]

In the current study we have demonstrated that the lifetime of the $CH_3S(O)(OH)CH_3$ adduct is less than 10 μs (at 298 K and 20 Torr). This upper limit on the $CH_3S(O)(OH)CH_3$ lifetime implies that under atmospheric conditions a reaction between the adduct and O_2 must have a rate coefficient of at least 10^{-14} cm^3 $molecule^{-1}$ s^{-1} to compete with adduct decomposition. However, it is very likely the rate coefficient for the $CH_3S(O)$-

$(OH)CH_3 + O_2$ reaction is significantly larger than 10^{-14} cm^3 $molecule^{-1}$ s^{-1} considering the $(1.0 \pm 0.3) \times 10^{-12}$ cm^3 $molecule^{-1}$ s^{-1} rate coefficient reported for the $CH_3S(OH)CH_3 + O_2$ reaction.[14,15] If the $CH_3S(O)(OH)CH_3 + O_2$ rate coefficient is on the order of 10^{-12} cm^3 $molecule^{-1}$ s^{-1}, then the $CH_3S(O)(OH)CH_3$ lifetime would have to be <0.5 μs for decomposition to be a significant pathway under atmospheric conditions. Unfortunately, the low DMSO vapor pressure (ca. 0.6 Torr at 298 K)[25] prohibits attainment of the experimental conditions necessary to observe a $CH_3S(O)(OH)CH_3$ lifetime $\lesssim 0.5$ μs (a CH_3 appearance rate of ca. 2 000 000 s^{-1} requires a [DMSO] roughly equal to the DMSO vapor pressure).

Under all experimental conditions, the CH_3 appearance rate was limited by the OH + DMSO reaction and not adduct decomposition. Our data define an upper limit for the adduct lifetime (at 20 Torr and 298 K), and we believe the true adduct lifetime is significantly less than 10 μs. With only an upper limit on the adduct lifetime and not a measurement of the actual adduct decomposition rate, it is difficult to speculate on how the adduct decomposition rate might vary with pressure. As discussed in the Experimental Section of this paper, the loss of signal sensitivity due to pressure broadening of the absorption features prevented us from conducting experiments at atmospheric pressures. If the CH_3 observed in the current study results from decomposition of an unthermalized adduct, i.e., reaction 1b, then adduct stabilization will be promoted at atmospheric pressure; however, if the observed CH_3 elimination is occurring via a thermalized adduct (reaction 2b), then decomposition may be accelerated at atmospheric pressure.

In an effort to more clearly establish the applicability of our results with respect to atmospheric conditions, we have begun experiments designed to measure (via UV absorption) the yield of CH_3OO from the OH + DMSO reaction in the presence of O_2. Preliminary experiments observing CH_3OO in the presence of varied $[O_2]$ (3−218 Torr) suggest that CH_3 elimination is the dominant reaction channel, even in the presence of atmospheric levels of O_2; however, the results are not yet sufficiently precise to rule out a minor but significant $CH_3S(O)(OH)CH_3 + O_2$ reaction channel under atmospheric conditions.[38]

Our proposed OH + DMSO reaction mechanism appears to be in contradiction with one finding of the Sorensen et al.[12] chamber study. Sorensen et al. employed an "off-line" ion chromatography technique for the measurement of MSIA. When the OH-initiated oxidation of DMS was studied, an MSIA yield of $1.5 \pm 1.1\%$ was measured. However, when studying the OH-initiated oxidation of DMSO, Sorensen et al. did not observe MSIA and reported an MSIA yield of $<0.3\%$ (below the limit of detection). Sorensen et al. have proposed that the MSIA observed in the OH-initiated oxidation of DMS may have resulted from the reaction of the $CH_3S(OH)CH_3$ adduct with O_2. Observation of MSIA in the OH-initiated oxidation of DMS, but not in the OH-initiated oxidation of DMSO, appears incompatible with our proposal that MSIA is the CH_3 coproduct of the OH + DMSO reaction. The explanation for the apparent discrepancy between our results and those of Sorensen et al. remains unclear. It is worth noting, however, that (a) about 50% of the sulfur product was unaccounted for in the Sorensen et al. study and (b) MSIA is expected to be quite reactive in both the vapor and condensed phases.

The OH-initiated oxidation of $CH_3S(O)(OH)$ may lead to the production of SO_2 in the remote marine environment. On the basis of the estimated BDEs and analogy to liquid-phase chemistry, Yin et al.[36] have suggested that OH may react with MSIA by abstraction of the hydroxyl H atom, producing $CH_3S(O)(O)$. Decomposition of $CH_3S(O)(O)$ would lead to SO_2, while further reaction of this species may generate SO_3 or methane sulfonic acid (MSA, $CH_3S(O)(O)(OH)$). The chamber studies of Barnes et al.[18] and Sorensen et al.[12] demonstrate that the OH-initiated oxidation of DMSO produces SO_2 (although there is an apparent major discrepancy between the two studies regarding the efficiency of SO_2 production). Additionally, the decomposition of $CH_3S(O)(O)$ to SO_2 and CH_3 has been observed in the low-pressure (ca. 1 Torr of He), room-temperature LIF−mass spectrometry study of Ray et al.[39] These studies lend strong support to the idea that the OH + DMSO reaction may lead to SO_2 production through the OH-initiated oxidation of MSIA.

Recent atmospheric field measurements in the marine boundary layer on the Antarctic coast suggest that the O_2-dependent branch of the OH-initiated oxidation of DMS is responsible for the production of gas-phase methane sulfonic acid ($CH_3S(O)(O)(OH)$, MSA), as well as being a major source of SO_2.[40] Observed MSA concentrations were consistent with the OH + DMSO reaction forming MSIA and the subsequent OH-initiated oxidation of MSIA leading, in part, to MSA production.[40] The results of our study are consistent with the OH-initiated oxidation of MSIA being both the source of MSA and a contributor to SO_2 production during the recent Antarctic field measurement campaign.

The efficiency with which DMSO oxidation may lead to MSA and SO_2 production will depend not only on the rate of MSIA oxidation by OH, but also on the ambient aerosol surface area, as DMSO and most likely MSIA are susceptible to physical removal. The interpretation of recent atmospheric field measurements on the Antarctic coast[40] and in the equatorial Pacific[41] suggest that heterogeneous removal of DMSO (and probably MSIA) is competitive with and may even dominate DMSO removal by reaction with OH.[42] Analysis of the field measurements taken in the Antarctic boundary layer suggest 60−80% of the DMSO in the lower troposphere is removed by heterogeneous processes,[40,42] whereas analysis of the equatorial Pacific field measurements indicate heterogeneous processes accounted for only 25−33% of DMSO removal.[41,42]

The results of our study suggest that the OH + DMSO reaction produces $CH_3S(O)(OH)$ and CH_3 in high yield. Methane sulfinic acid may be a key species whose OH-initiated oxidation may lead to production of MSA and SO_2. The role of MSIA in atmospheric sulfur chemistry will likely be most important at high latitudes where the O_2-dependent branch of the OH + DMS reaction dominates overall DMS reactivity. Direct observation of gas-phase MSIA as a product of the OH + DMSO reaction (in the presence of O_2) is necessary to thoroughly confirm the interpretation of our results and to clear up the discrepancy between the current study and the chamber study of Sorensen et al.[12] The ability to directly observe MSIA in the gas phase is also necessary to conduct time-resolved kinetic and product studies of the potentially important OH + MSIA reaction.

Acknowledgments. This research was supported by the National Science Foundation under Grant No. ATM-94-12237. Shawn P. Urbanski was supported by the NASA Earth System Science Fellowship Program. The authors thank D. Davis and G. Chen for sharing their results prior to publication and for helpful and insightful discussions regarding atmospheric sulfur chemistry.

References and Notes

(1) Berresheim, H.; Wine, P. H.; Davis, D. D. In *Composition, Chemistry and Climate of the Atmosphere*; Singh, H. B., Ed.; Van Nostrand Rienhold: New York, 1995; pp 251−307 and references therein.

(2) Bates, T. S.; Lamb, B. K.; Guenther, A.; Dignon, J.; Stoiber, R. E. *J. Atmos. Chem.* **1992**, *14*, 315.
(3) Spiro, P. A.; Jacob, D. J.; Logan, J. A. *J. Geophys. Res.* **1992**, *97*, 6023.
(4) Jonas, P. R.; Charlson, R. J.; Rodhe, H. In *Climate Change 1994. Radiative Forcing of Climate Change*, Intergovernmental Panel on Climate Change, Eds.; Cambridge University Press: Cambridge, 1995; pp 133−157 and references therein.
(5) Shaw, G. E. *Clim. Change* **1983**, *5*, 297.
(6) Charlson, R. J.; Lovelock, J. E.; Andreae, M. O.; Warren, S. G. *Nature* **1987**, *326*, 655.
(7) Berresheim, H.; Eisele, F. L.; Tanner, D. J.; McInnes, L. M.; Ramsey-Bell, D. C.; Covert, D. S. *J. Geophys. Res.* **1993**, *98*, 12701.
(8) Bandy, A. R.; Thornton, D. C.; Blomquist, B. W.; Chen, S.; Wade, T. P.; Ianni, J. C.; Mitchell, G. M.; Nadler, W. *Geophys. Res. Lett.* **1996**, *23*, 741.
(9) Berresheim, H.; Huey, J. W.; Thorn, R. P.; Eisele, F. L.; Tanner, D. J.; Jefferson, A. *J. Geophys. Res.* **1998**, *103*, 1629.
(10) Barnes, I.; Becker, K. H.; Patroescu, I. *Geophys. Res. Lett.* **1994**, *21*, 2389.
(11) Barnes, I.; Becker, K. H.; Patroescu, I. *Atmos. Environ.* **1996**, *30*, 1805.
(12) Sørensen, S.; Falbe-Hansen, H.; Mangoni, M.; Hjorth, J.; Jensen, N. R. *J. Atmos. Chem.* **1996**, *24*, 299.
(13) Hynes, A. J.; Wine, P. H.; Semmes, D. H. *J. Phys. Chem.* **1986**, *90*, 4148.
(14) Hynes, A. J.; Stoker, R. B.; Pounds, A. J.; McKay, T.; Bradshaw, J. D.; Nicovich, J. M.; Wine, P. H. *J. Phys. Chem.* **1995**, *99*, 16967.
(15) Barone, S. B.; Turnipseed, A. A.; Ravishankara, A. R. *J. Phys. Chem.* **1996**, *100*, 14694.
(16) Hynes, A. J.; Stickel, R. E.; Pounds, A. J.; Zhao, Z.; McKay, T.; Bradshaw, J. D.; Wine, P. H. In *Dimethylsulphide: Oceans, Atmosphere, and Climate*; Restelli, G., Angelletti, G., Eds.; Kluwer Academic Publishers: London, 1993; pp 211−221.
(17) Turnipseed, A. A.; Barone, S. B.; Ravishankara, A. R. *J. Phys. Chem.* **1996**, *100*, 14703.
(18) Barnes, I.; Bastian, V.; Becker, K. H.; Martin, D. In *Biogenic Sulfur in the Environment*; ACS Symposium Series 393; American Chemical Society: Washington, DC, 1989; pp 476−488.
(19) Hynes, A. J.; Wine, P. H. *J. Atmos. Chem.* **1996**, *24*, 23.
(20) Stickel, R. E.; Nicovich, J. M.; Wang, S.; Zhao, Z.; Wine, P. H. *J. Phys. Chem.* **1992**, *96*, 9875.
(21) Stickel, R. E.; Chin, M. E.; Daykin, E. P.; Hynes, A. J.; Wine, P. H.; Wallington, T. J. *J. Phys. Chem.* **1993**, *97*, 13653.
(22) Zhao, Z.; Stickel, R. E.; Wine, P. H. *Chem. Phys. Lett.* **1996**, *251*, 59.
(23) Urbanski, S. P.; Stickel, R. E.; Zhao, Z.; Wine, P. H. *J. Chem. Soc., Faraday Trans.* **1997**, *93*, 2813.
(24) DeMore, W. B.; Sander, S. P.; Golden, D. M.; Hampson, R. F.; Kurylo, M. J.; Howard, C. J.; Ravishankara, A. R.; Kolb, C. E.; Molina, M. J. *Chemical Kinetics and Photochemical Data for Use in Stratospheric Modeling*; JPL Publication 94-26; Jet Propulsion Laboratory: Pasadena, CA, 1994.
(25) Douglass, T. B. *J. Am. Chem. Soc.* **1948**, *70*, 2001.
(26) Yamada, C.; Hirota, E.; Kawaguchi, K. *J. Chem. Phys.* **1981**, *75*, 5256.
(27) Brown, L. R.; Farmer, C. B.; Rinsland, C. P.; Toth, R. A. *Appl. Opt.* **1987**, *26*, 5154 and references therein.
(28) (a) Nicovich, J. M.; Van Dijk, C. A.; Kreutter, K. D.; Wine, P. H. *J. Phys. Chem.* **1991**, *95*, 9890. (b) Seakins, P. W.; Pilling, M. J.; Niiranen, J. T.; Gutman, D.; Krasnoperov, L. N. *J. Phys. Chem.* **1992**, *96*, 9847.
(29) (a) Roehl, C. M.; Burkholder, J. B.; Moortgat, G. K.; Ravishankara, A. R.; Crutzen, P. J. *J. Geophys. Res.* **1997**, *102*, 12819. (b) Rattigan, O. V.; Shallcross, D. E.; Cox, R. A. *J. Chem. Soc., Faraday Trans.* **1997**, *93*, 2839.
(30) Zhao, Z.; Stickel, R. E.; Wine, P. H. *Geophys. Res. Lett.* **1995**, *22*, 615.
(31) Clyne, M. A. A.; Whitefield, P. D. *J. Chem. Soc., Faraday Trans. 2*. **1979**, *75*, 1327.
(32) Brunning J.; Stief, L. J. *J. Chem. Phys.* **1986**, *84*, 4371.
(33) Sivakumar, N.; Hall, G. E.; Houston, P. L.; Hepburn, J. W.; Burak, I. *J. Chem. Phys.* **1988**, *88*, 3692.
(34) (a) Black, G.; Jusinski, L. E. *J. Chem. Phys.* **1985**, *82*, 789. (b) Black, G. *J. Chem. Phys.* **1986**, *84*, 1345. (c) McBane, G. C.; Burak, I.; Hall, G. E.; Houston, P. L. *J. Phys. Chem.* **1992**, *96*, 753.
(35) Addison, M. C.; Byrne, C. D.; Donovan, R. J. *Chem. Phys. Lett.* **1979**, *64*, 57.
(36) Yin, F.; Grosjean, D.; Seinfeld, J. H. *J. Atmos. Chem.* **1990**, *11*, 309.
(37) Hynes, A. J.; Wine, P. H. In *Combustion Chemistry*, 2nd ed.; Gardiner, W. C., Ed.; Springer-Verlag: New York, in press.
(38) Urbanski, S. P.; Wine, P. H. Unpublished data.
(39) Ray, A.; Vassalli, I.; Laverdet, G.; Le Bras, G. *J. Phys. Chem.* **1996**, *100*, 8895.
(40) Davis, D.; Chen, G.; Kasibhatla, P.; Jefferson, A.; Tanner, D.; Eisele, F.; Lenschow, D.; Neff, W.; Berresheim, H. *J. Geophys. Res.* **1998**, *103*, 1657.
(41) Davis, D.; Chen, G.; Bandy, D.; Thornton, D.; Eisele, F.; Mauldin, L.; Tanner, D.; Lenschow, D.; Fuelberg, H.; Huebert, B.; Heath, J.; Clarke, A.; Blake, D. *J. Geophys. Res.* **1998**, submitted for publication.
(42) Davis, D.; Chen, G. Personal communication, 1998.